frontiers | Frontiers in Built Environment

TYPE Original Research
PUBLISHED 02 March 2023
DOI 10.3389/fbuil.2023.1119696

OPEN ACCESS

EDITED BY
Eugenia Gasparri,
The University of Sydney, Australia

REVIEWED BY
Marina Bonomolo,
University of Palermo, Italy
Piercarlo Romagnoni,
Università Iuav di Venezia, Italy

*CORRESPONDENCE
Nimish Biloria,
nimish.biloria@uts.edu.au

SPECIALTY SECTION
This article was submitted to Sustainable Design and Construction, a section of the journal Frontiers in Built Environment

RECEIVED 09 December 2022
ACCEPTED 02 February 2023
PUBLISHED 02 March 2023

CITATION
Biloria N, Makki M and Abdollahzadeh N (2023), Multi-performative façade systems: The case of real-time adaptive BIPV shading systems to enhance energy generation potential and visual comfort. *Front. Built Environ.* 9:1119696. doi: 10.3389/fbuil.2023.1119696

Multi-performative façade systems: The case of real-time adaptive BIPV shading systems to enhance energy generation potential and visual comfort

Nimish Biloria[1,2]*, Mohammed Makki[1] and Nastaran Abdollahzadeh[1]

[1]Faculty of Design Architecture and Building, School of Architecture, University of Technology Sydney, Sydney, NSW, Australia, [2]Department of Urban and Regional Planning, Faculty of Engineering and the Built Environment, University of Johannesburg, Johannesburg, South Africa

Building envelopes invariably tend to be static systems that encounter various performance limitations such as inefficient illuminance admittance, and heat and moisture transmission owing to their non-responsiveness towards environmental fluctuations. In contrast to such façade solutions, responsive façade systems with embedded sensing, actuation, and control systems have been proven to perform with up to 65% higher efficiency by being able to adapt their physical characters, such as orientation, and material property in real-time as a response to fluctuating environmental conditions (visual and thermal) and user preferences. Advancements in artificial intelligence and machine learning processes further aid such responsive façade systems to optimize multiple parameters such as illuminance level and the associated lighting energy, visual discomfort caused by solar glare, solar heat gain, thermal resistance (heating energy and comfort level), and natural ventilation simultaneously. This research investigates the case of a real-time adaptive Building Integrated Photo Voltaic (BIPV) shading system and its ability (in comparison with traditional static building integrated photo voltaic façade systems) to perform as regards visual comfort and energy generation potential simultaneously within the humid subtropical climate of Sydney, Australia. A simulated case scenario wherein a real-time adaptive building integrated photo voltaic shading systems is deployed on a typical multistorey building façade in Sydney, Australia is accordingly presented. The conducted simulation considers the responsive building integrated photo voltaic system as a double-skin façade system and uses multi-objective evolutionary computing principles to decipher its integrability potential. A comparative analysis between traditional static mounted Photo Voltaic (PV) systems as opposed to multi-objective optimization driven real-time adaptive building integrated photo voltaic shading configurations is subsequently presented. The ability to maximize generated energy, while simultaneously maintaining visual comfort is thus a unique proposition of this research.

KEYWORDS

real-time adaptive BIPV systems, double-skin facade, architecture, climate change, multi-performative design, multi-objective evolutionary optimization, resource efficiency, energy generation

1 Introduction

The building and the construction sector are responsible for 32% of the global energy consumption and 37% of greenhouse gas emissions, respectively. Residential and commercial buildings alone account for 30% of the final energy consumption (International Energy Agency and the United Nations Environment Program, 20121). Simultaneous, population growth and the exponential rate of urbanization further increases the demand for energy consumption, resulting in adverse environmental impacts (Yang et al., 2020). Dense urban patterns incorporating high-rise buildings as a means to cater to this population growth further increases the amount of energy consumed for heating and cooling purposes (Abdollahzadeh and Biloria, 2022). It is expected that the energy use and associated environmental pollutant emissions that impact public health are set to double or even tripled by the mid of the 21st century (International Energy Agency, 2013). Planetary health and environmental concerns have thus undoubtedly become common concerns globally (Yang et al., 2020), resulting in an urgency around the development of preventative mitigation measures to be considered for countering human-induced climate change (Secretariat, 2015). A paradigm shift embracing the large-scale implementation of renewable energy sources is thus quintessential.

In this context, apart from building new, energy efficient buildings, the potential for energy and Carbon dioxide (CO_2) mitigation (up to 50%–90%) of existing, non-energy efficient building stock (Lucon and Ürge-Vorsatz, 2014; Biloria and Abdullahzadeh, 2022) by adopting clever means of retrofitting cannot be undermined. In Australia, commercial buildings consume 10% of the national energy out of which 25% is consumed by office buildings (Council of Australian Governments, 2012; Ernst and Young, 2016). According to the International Energy Agency (IEA), global renewable power capacity shall increase by 50% in 2024 (since 2019) (IEA, 2019). Solar PV systems will constitute 60% (equivalent to 1200 Giga Watt) of this increased renewable power generation capacity (Poon et al., 2020). Energy retrofitting of existing buildings is thus deemed a potential solution to address this energy demand and BIPVs can be specifically used as a net-positive energy tool in this regard.

A buildings' façade is a crucial element that can impact energy consumption, presenting itself as an excellent element for building retrofitting. The façade acts as a connecting element between the indoor and the outdoor environment, thus affecting heating, cooling, and lighting conditions significantly. This in-turn influences the amount of energy consumed for satisfying comfort conditions in the interiors of buildings. Thermal fluxes through a building's envelope can further influence heating and cooling loads. One mitigation measure for such façade traits is a double skin façade system (DSF) with building integrated photo voltaic systems (BIPV). A double skin façade (DSF) can greatly improve the performance of building facades with respect to maintaining optimal thermal comfort and energy savings simultaneously. Such facade systems have the capability to control the amount of daylight received in interiors, solar heat gain, ventilation, and thermal exchange through a building's envelope (Lee et al., 2002).

Typical DSFs consist of an external glazed skin and a ventilated cavity with operable vents between the main envelope and the exterior skin facade. A high rate of ventilation through the cavity (open vents) in summer and minimum ventilation in winter (closed vents) increases thermal comfort and enhances a building's environmental performance. This ventilation it helps BIPVs in thermal washing: cooling of building elements in contact with the cavity thus increasing the efficiency of PV panels (Agathokleous and Kalogirou, 2016; Yang and Athienitis, 2016; Prieto et al., 2019). According to Agathokleous and Kalogirou (2016), DSFs should be able to provide a comfortable indoor climate, sound protection, use of daylighting while minimizing energy demand simultaneously. In this configuration, BIPV facade systems, not only generate extra electricity; but also protect the building's envelope against excessive heat transfer. PV installation on roofs and facades have the potential to exceed the local non-baseload demand and fulfill 50%–75% requirements of the total energy use (Karava et al., 2012).

The following sections further elaborates upon the role of BIPVs for climate conscious retrofitting.

2 Building integrated photovoltaics (BIPVs) as a climate conscious retrofitting solution

BIPV facade systems can be used as a retrofitting solution (Eicker et al., 2015; Evola and Margani, 2016; Hachem et al., 2014) to enhance the appearance and performance of existing buildings, resulting in material and energy savings simultaneously (Martín-Chivelet et al., 2018). According to Martin-Chivelet et al. (2018), PV panels can be easily integrated into the building envelope at a competitive cost (Delponte et al., 2015), and their characteristics can be coherent with the overall building's design in terms of architectural composition, colors, and textures (Martín-Chivelet et al., 2018). Additionally, their lightweight and flexible nature allow for easy integration into building facades (Yu et al., 2021). Also, developments in thin-film BIPV technology in terms of their efficiency and cost effectiveness have made their integration into novel architectural designs with complex geometry feasible (Jelle et al., 2012; Kaelin et al., 2004; Kushiya, 2014; Wilson, 2015). It can thus be argued that "high electrical efficiency, low cost, and the ease of installation are key to the wide acceptance and adoption of BIPV" systems (Yu et al., 2021), for addressing growing energy demands (Defaix et al., 2012; Raugei and Frankl, 2009). Local electricity generation using eliminate losses incurred during energy transportation, thus proving to be more cost-effective. BIPV as a double skin façade also offers acoustic benefits. Improving aesthetics and ease of installation are the other features that can be considered as advantages that BIPV elements offer, especially for retrofitting and renovation purposes (Biyik et al., 2017).

BIPV facade systems have been studied in different climatic contexts, including South Korea (Joe et al., 2013), Hong Kong (Peng et al., 2013; Peng et al., 2016), etc., however, very few studies have been conducted in the southern hemisphere, and subtropical or temperate climates. Within these limited studies, a study by Joe et al. (2013) suggests that a BIPV facade system reduces heating and cooling energy use by 16% and 7%, respectively (Joe et al., 2013). However, a later study, also indicates a 51% solar heat gain in

TABLE 1 Thermal properties of "naturally-ventilated BIPV/T-DSF" system (Australian Building Codes Board, 2016).

Parameters	Naturally ventilated BIPV/T-DSF	Requirement of the local regulation
U-value of the external wall (W/m2K)	0.51	Climate zone 1, 2, and 3: U ≥ 0.3
		Climate zone 4, 5, 6, and 7: U ≥ 0.36
		Climate zone 8: U ≥ 0.26
U-value of external roof (W/m2K)	0.316	Climate zone 1, 2, 3, 4, 5, and 6: U ≥ 0.31
		Climate zone 7: U ≥ 0.27
		Climate zone 8: U ≥ 0.21
Floor—a slab on the ground (boundary condition)	Adiabatic	N/A
U-value of internal window (W/m2K)	5.68	Climate zone 1, 2, and 3: 5.0 ≤ U ≤ 7.9
		Climate zone 4 and 5: 3.5 ≤ U ≤ 7.0
		Climate zone 6, 7, and 8: 3.0 ≤ U ≤ 6.0
Solar transmittance of internal window	83%	N/A
Solar reflectance of internal window	7.5%	N/A

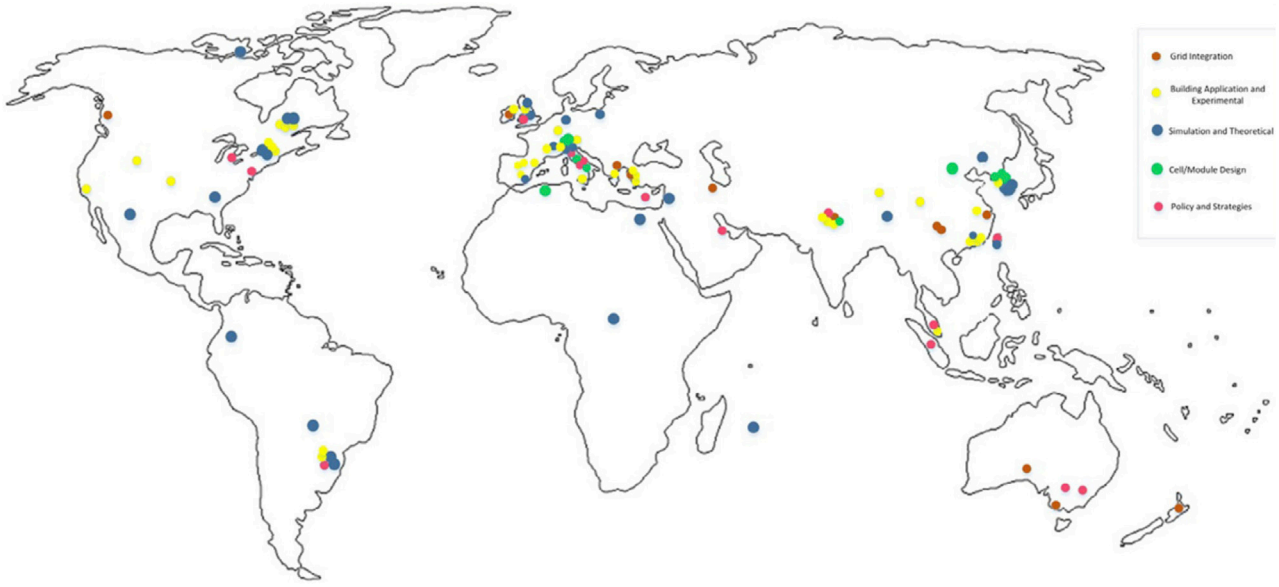

FIGURE 1
Worldwide studies on BIPV systems (Biyik et al., 2017).

summer and 32% heat loss in winters through such systems (Peng et al., 2013). Fossa et al. (2008) also investigated the thermal behavior of the BIPV/T-DSF system in Sydney (Australia) in a climatic context like this study (Fossa et al., 2008). Nevertheless, Fossa et al.'s study only reports on indoor environment tests (Yang et al., 2020). Australian building codes board also offers certain thermal properties for external envelope construction (naturally ventilated BIPV/T-DSF) to control heat loss and gain, which directly affects the energy demand of buildings (Australian Building Codes Board, 2016). These values are summarized in Table 1.

Furthermore, a comparative study on double skin facades with integrated BIPV technologies by Heidari Matin and Eydgahi, indicate that such efficient facade systems typically offer 30% improvement in visual comfort, and a 50% and 20% reduction in energy use values and carbon emissions, respectively. Moreover, an 80% reduction in thermal loads and a 25% reduction in cooling loads are reported (Heidari Matin and Eydgahi, 2019), which results in 15%–20% (cooling) cost efficiency respectively (Kolarevic and Parlac, 2015). Figure 1 indicates the studies conducted on BIPV worldwide (till 2017), according to a review conducted by Biyik et al., 2017. Figure 1 also categorizes the nature of conducted studies into five categories: Grid integration, Building

application and experimental, Simulation and theoretical, Cell/Module design, and Policy and Strategies.

According to a review conducted by Agathokleous and Kalogirou (2016), to keep the BIPV temperature at a low level through natural ventilation, an optimal air gap of 10–15 cm between the PV panels and the building envelope (Agathokleous and Kalogirou, 2016) should be maintained. However, they also suggest that depending on the climatic condition and ventilation rate, the width of this air gap and the associated efficiency of the modules can be increased. In a study conducted by Martín-Chivelet et al., 2018, facade ventilation caused an annual 2.5% increase in the efficiency of PV panels as compared to a non-ventilated facade. An increase in temperature could however also result in a 3% decrease in the obtained power (Martín-Chivelet et al., 2018). A recent study by Goncalves et al. (2020) also employs the sensitivity analysis (SA) method along with computational simulation to explore the performance of naturally ventilated BIPV facade systems. The study reported exterior convective heat transfer coefficient to be the most influential factor impacting the performance of BIPV systems. The study also indicates that cavity ventilation can become more important when the exterior convective heat transfer decreases. Furthermore, solar irradiance is also found to be a vital factor affecting BIPV power outputs (Gonçalves et al., 2020).

2.1 The multifunctional use-case of BIPV façade systems

BIPV systems can be more cost-effective when they offer more than one function besides power generation. Some such functions include BIPVs acting as shading systems and promoting active solar heating and lighting (Agathokleous and Kalogirou, 2016; Farkas et al., 2013; Bonomo et al., 2015; Agathokleous and Kalogirou, 2016). According to Agathokleous and Kalogirou, thermal buffer zones, solar preheating of ventilated air, sound protection, wind and pollutant protection, night cooling and space for energy collection devices like PV cells are some of the use cases that can be considered when designing double skin facades as a cost-effective material substitute for buildings envelopes (Agathokleous and Kalogirou, 2016). Besides this, BIPVs can also act an insulation layer, a weather barrier, or a sun shading system (Gonçalves et al., 2020; Quesada et al., 2012).

Such multi-functionality of BIPV's is thus ideally suited for improving power generation as well as enhancing thermal comfort, natural lighting, heating, cooling, etc., (Yoo, 2011). They are also ideal for acting as an element of a double façade building envelope - serving as insulator during the night besides generating energy during the day. This use-case scenario is tested in a study by Yoo and Manz (2011) using SOLCEL, a photovoltaic system analysis program (Yoo and Manz, 2011). This computational method is also used in a later study of theirs with a focus on the position of the PV panels as shading devices to maximize power generation in the climatic context of the Suwon area, Korea. The findings of this study indicate that south/east (at 50°, building azimuth 130°) and south/west (at 50°, building azimuth 230°) offered a higher energy generation capacity compared to the exact south. A considerable impact of the PV's angle, building azimuth, and albedo on the power generation potential of BIPVs is thus reported in an evidence-based manner (Yoo, 2011). The use-case of BIPV window system design is, however, more sensitive as a minimum amount of transparency is required in windows, and PV films offer acceptable SHG value for this purpose. According to a study by Cannavale et al. (2017) in southern Italy, BIPV windows with shading systems have the potential to reduce the overall annual energy use by 18% compared to standard clear glass windows (Cannavale et al., 2017).

A study in the Australian contexts investigating the performance of building-integrated photovoltaic/thermal double-skin facade (BIPV/T-DSF) reported a total annual energy savings of 34.1%, 86%, and 106% annually could be attained in Darwin, Sydney, and Canberra, when compared with conventional technologies. This study explored different design parameters such as cavity depth of a double skin facade, rate, and mode of ventilation (natural vs. mechanical), thermal transmittance, and the opening ratio of ventilation louvers, to decipher impacts on heating and cooling loads and associated energy consumption of buildings through a sensitivity analysis. Although an additional energy saving is predicted for mechanically ventilated DSFs (lowest cooling energy use), non-ventilated DSFs offered the lowest heating energy use in the subtropical climate zone of Australia (Yang et al., 2020). A review conducted by Agathokleous and Kalogirou, suggest further research is vital to extrapolate advantages and effective usage of BIPVs (Agathokleous and Kalogirou, 2016).

A vital use-case for BIPV systems takes up the form of shading devices. The following section examines the application of BIPV's as facade shading systems when they are deployed in fixed, tilted, and adaptive configurations.

2.2 BIPV as shading systems

A study by Jayathissa et al. (2017) classifies previous research on BIPV shading systems in two categories: The effects of BIPV on building energy performance, and the integration of building energy performance simulation with shading systems (Jayathissa et al., 2017). PV integrated louvers used for shading result in significant energy savings, especially when used for cooling in hot climatic conditions (Palmero-Marrero and Oliveira, 2010). A tilted BIPV louver can typically generate 20%–40% more electricity than a flat vertical one (Freitas and Brito, 2015), and can reduce cooling demand by up to 51.6% (Sun et al., 2012).

Another shading system design in Denmark indicates the efficiency of dynamic shading systems over static/fixed ones (Nielsen et al., 2011). An adaptive shading system can control both solar heat gain and lighting conditions, thus improving a buildings' performance in terms of energy use, and thermal and visual comfort simultaneously. Such BIPV shading system can thus increase visual comfort, and prevent excessive solar radiation, thus reducing the need for excessive energy spending for cooling during summer while providing sufficient solar access during winter for passive heating (Yu et al., 2021). On a sunny winter and summer day, adaptive solar facades (ASFs) can compensate for 62% and 270% of the energy demand of buildings in the climatic context of Zurich, and Switzerland (Jayathissa et al., 2017). While in Los Angeles, the annual HVAC energy reduction is reported to be 30% using thin-film PV on glazed surfaces (Chae et al., 2014).

Such adaptive systems can also affect the thermal and optical condition of interiors. ASF's as dynamic systems continuously adapt to solar geometry to control direct and indirect radiation penetration into the buildings and thus reduce net HVAC loss (caused by less solar heat gain in colder climates (Chae et al., 2014), while increasing occupant comfort simultaneously (Loonen et al., 2013).

BIPV adaptive shading systems can thus supply the electricity required for heating, cooling, and lighting simultaneously (Jayathissa et al., 2017). A recent study by Yu et al. (2021) investigates three different categories of 'outdoor PV blinds, indoor PV blinds and middle PV blinds' (named based on the position of blinds relative to the windows). The study concluded that BIPV blinds are easier to adjust compared to BIPV windows and are thus more efficient in terms of energy generation and solar heat gain. Additionally, double-glazed BIPV shading blinds could perform better in winters compared to double glazing (semi-transparent façade) due to a higher solar heat gain coefficient (SHGC) and lower U-value (Yu et al., 2021). Another study on movable BIPV sun-shading systems installed on windows indicates that the thermal load of buildings can be reduced by up to 16% while electricity generation can be increased by 70% as compared to a fixed BIPV system as a secondary skin facade (Paydar, 2020).

Different studies are conducted on outdoor (Bahr, 2014; Park et al., 2016; Vadiee et al., 2016; Gao et al., 2018; Taveres-Cachat et al., 2019; Paydar, 2020), middle (Kang et al., 2012; Luo et al., 2018; Luo et al., 2017; Hong et al., 2017; Jeong et al., 2017; Koo et al., 2017), and indoor (Davidsson et al., 2010; Davidsson et al., 2012) BIPV shading blinds. Results of these studies suggested that middle PV blinds have the potential of energy savings up to 12.2% and 25.6% compared to traditional double-glazed windows or windows without blinds (Luo et al., 2017). The application of outdoor shading blinds is however limited due to their high costs. However, where external shadings are appropriate to install, outdoor PV blinds would also exhibit potential benefits (Yu et al., 2021). Jayathissa et al. (2017), conducted a similar study on dynamic photovoltaic systems for adaptive shading purposes to optimize the orientation of PV shading panels for maximum energy generation and minimizing heating, cooling, and lighting demand in office interiors. The finding indicates a 20%–80% energy saving (compared to static PV shadings), and that a 90° and 15°–45° (to the vertical plane) angle are required for the adaptive solar facade (ASF) to perform most efficiently. Moreover, PV generated energy supply can compensate for the annual energy demand by up to 95%, if an efficient HVAC system is installed simultaneously (Coefficient of performance: 6) (Jayathissa et al., 2017).

Considering such scientific evidence, and increasing climate emergencies, this research further elaborates upon a case study undertaken by the authors. Dewidar et al claim that responsive façade systems have been proven to perform with up to 65% higher efficiency (Dewidar et al., 2010) by being able to adapt their physical characters, such as orientation, and material property in real-time as a response to fluctuating environmental conditions (visual and thermal) and user preferences. The study pertains to a real-time adaptive BIPV shading system installed as a double skin facade on an educational institute building in Sydney, Australia. The study explores the real-time adaptive nature of a BIPV double skin set-up as a plausible energy retrofit solution within the subtropical climate of Sydney. The retrofit solution is seen from a multi-performative perspective wherein its ability to maximize generated energy, while simultaneously increasing visual comfort is put to the test. The real-time adaptive nature of the proposed system implies the BIPV panels to augment their physical position in real-time based on the sun angle throughout the day. A multi-objective optimization driven computational process is deployed for simulating such adaptivity of the BIPV panels. A comparison between a static BIPV panel system vs. the proposed real-time adaptive panel system is subsequently conducted to reveal the advantages of the proposed system, thus adding a novel unexplored dimension of real-time adaptive BIPV systems to the knowledge base of BIPV façades.

3 Methodology

3.1 Multi-objective evolutionary algorithm for real-time adaptive BIPV systems

Multi-objective evolutionary algorithms mimic the natural cycle of an evolutionary process in which a base phenotype (the geometry that the algorithm will act on) is developed through a defined set of variables (genes). A MOEA incrementally "mutates" (varies) the genes that define the phenotype to create a generation of solutions; at the end of each generation, the algorithm evaluates the evolved solutions and retains the "successful" solutions and discards the "unsuccessful" solutions; this process forms the fundamental workflow of all evolutionary algorithms (De Jong, 2006). In the algorithmic process, "success" is defined by a numeric fitness function that each solution is tested against; if the applied genetic mutation results in an improvement of a solution's fitness function, it is retained, and if the mutation results in a worsening of the solution's fitness function, it is discarded. The genes of the retained solutions cross over with one another to create the next-generation; as more and more "fit" solutions are selected and cross over with each other, each subsequent generation evolved by the algorithm is comprised from solutions with higher fitness values.

One of the main advantages of an MOEA is that the designer can integrate multiple conflicting fitness functions to evaluate each solution simultaneously, thus allowing the algorithm to evolve a population of solutions that have been independently optimized to the different fitness functions (through the continuous minor improvement of solutions through incremental mutations), consequently generating a varied population of optimized phenotypes. MOEAs have been used extensively across multiple disciplines since the mid-20th century; with a sharp increase in their use within Architecture and Design in the past decade due to the proliferation of various MOEA tools within mainstream 3d modeling software (Showkatbakhsh and Mohammed, 2022).

Considering the aforementioned advantages, a MOEA is thus employed in this study to optimize the BIPV configurations in response to simultaneously satisfy three objectives: To maximize irradiance value on the BIPV, minimize internal illuminance values above 3000 lux, and minimize internal illuminance levels below 300 lux. The use of an MOEA allows for the optimization of conflicting objectives, which in the case study presented herein is

FIGURE 2
UTS Tower (Wpcpey, 2017), located in the city of Sydney is used as the base model for the presented experiment.

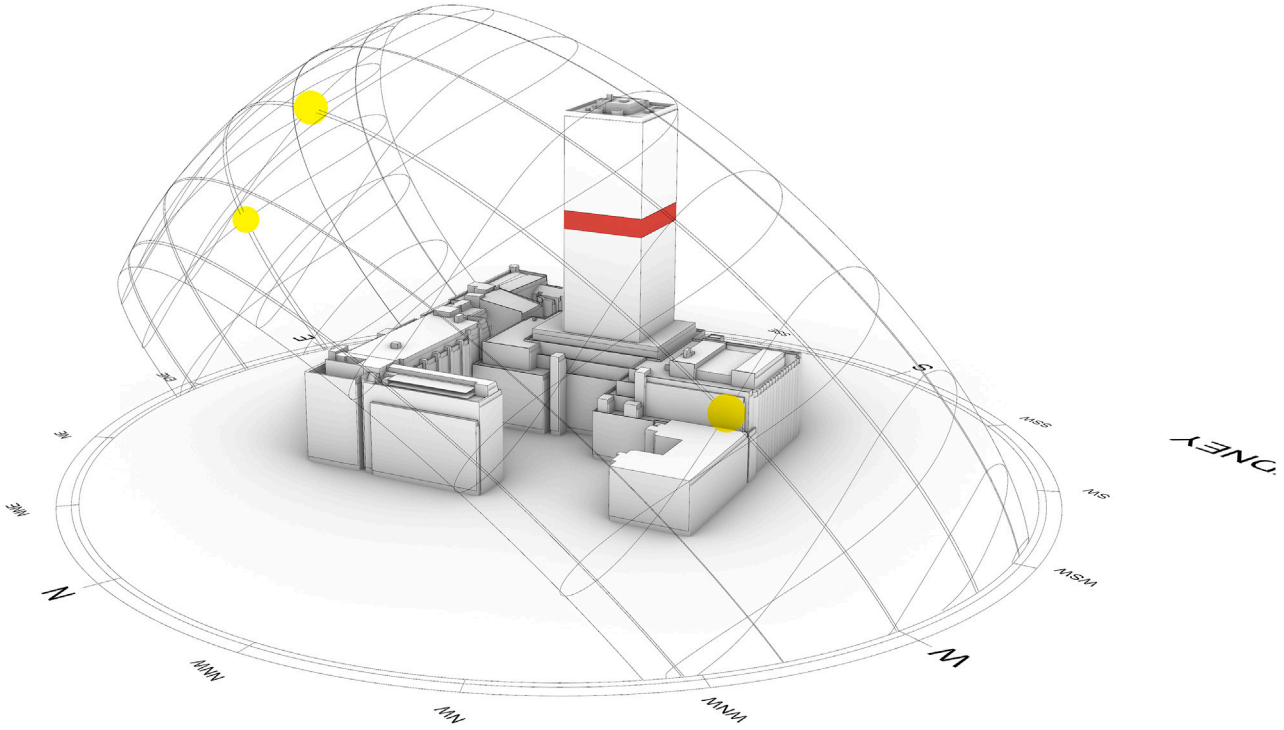

FIGURE 3
Solar analysis conducted for three different times of the day: March equinox (21st of March): 8:00am, 12:00pm and 4:00pm.

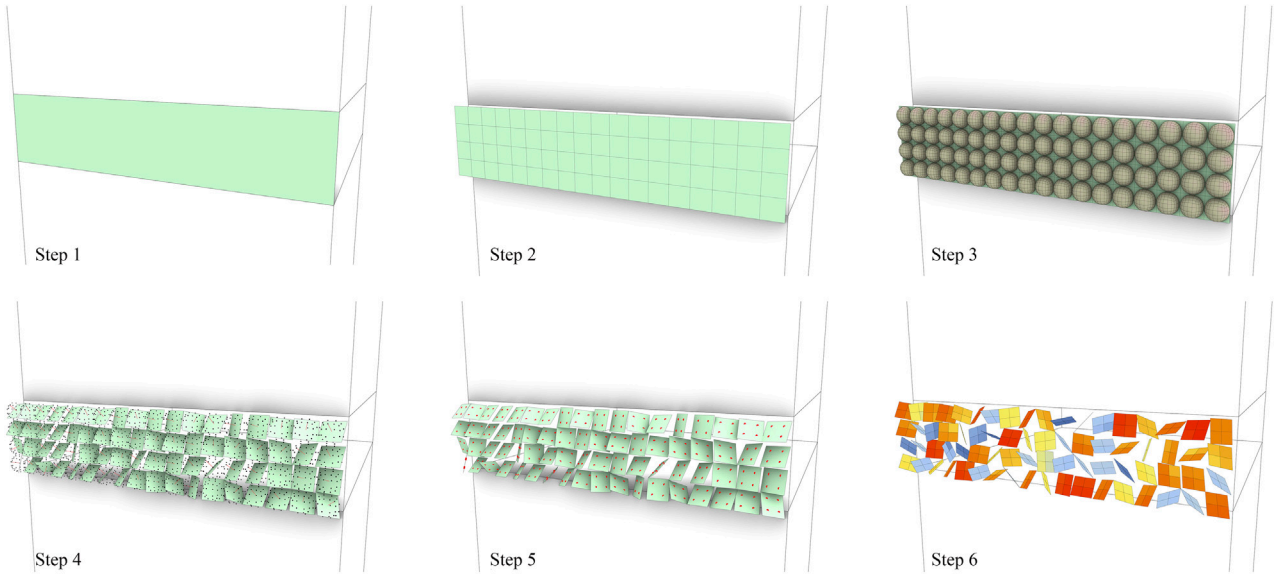

FIGURE 4
The step-by-step construction of the photovoltaic panels in the primitive phenotype.

critical to ensure the efficiency of the BIPVs is maximized with minimal intervention on the visual discomfort of the internal spaces, since the BIPV system is supposed to act as an energy generator and a shading device simultaneously. Moreover, due to the exponential number of possible configurations of the BIPV, utilizing an MOEA avoids the need to identify, model, and evaluate every possible configuration manually. This simultaneous multi-optimization of three objectives in an automated manner to develop real-time adaptive BIPV systems is thus seen as a novel contribution of this research.

3.2 Case study setup

The presented experiment selects a typical high-rise building in the city of Sydney: in this case, the University of Technology Sydney, Australia's Tower (Figure 2), and extracts two levels from the tower to run the MOEA. Selecting a section of the tower rather than the entire tower was primarily owing to the excessive runtime of the algorithm and the computational load associated with calculating irradiance. For the purpose of the presented study, conducting the analysis on a section of the tower is deemed sufficient as it allows for a comparative analysis between the algorithmic results and current approaches. The study presents three simulations, each optimizing the adaptive system for a different time of day during the March equinox (21st of March); 8: 00 a.m., 12:00 p.m., and 4:00 p.m. (Figure 3).

The base phenotype for the experiment consists of 72 photovoltaic panels, each one approximately 2 m × 2 m in size, distributed across two levels of the tower's northern facade. A single chromosome, comprising 72 unique genes, controls the orientation of each panel, with a freedom of movement of 180° (Figure 4). The phenotype is optimized against three fitness functions; the first maximizes the irradiance value on the photovoltaic cells, where each cell is divided into 4 sample points for the irradiance calculation. The other two objectives evaluate interior illuminance levels out of Useful Daylight Illuminance (UDI Autonomous) bonds (300–3000 lux), as this range provides desirable visual conditions (A. Chi et al., 2018): The second fitness function minimizes the percentage of the internal space (in the two selected levels) with an illuminance value above 3000 lux (as a lux value above this level is not recommended for internal spaces and increases glare probability), the third fitness function minimizes the percentage of internal space with an illuminance value below 300 lux. For the second and third fitness functions, the internal space (Figure 5A) is divided into a 1.2m grid (Figure 5B) for calculating the illuminance levels (Figure 5C).

The computational process involves two steps: First, all three simulations are conducted using the software Wallacei (Makki et al., 2018) inside the Rhino 3D and Grasshopper 3D ecosystem, which employs a non-dominated sorting genetic algorithm (NSGA-2) algorithm (Deb et al., 2000), Second, solar analyses of irradiance and illuminance utilizes the software Honeybee, also situated within the same ecosystem (Roudsari and Mackey, 2012). The simulation settings and algorithm properties are detailed in Table 2.

4 Results

Each simulation evolved 4900 solutions across 140 generations. As can be observed in the charts in Figure 6, which present the algorithm's progress in the optimization process for each fitness function separately, the 8 a.m., simulation was successful in optimizing for both maximizing irradiance on panels and minimizing illuminance values of the internal space below 300 lux. Due to the position of the solar vector at this time of the day, it was not possible for illuminance values to go over 3000 lux and thus that fitness function remained at 0. The results for the 12 p.m. simulation and 4 p.m. simulation share similar patterns of behavior, both of which differ from the 8 a.m. simulation. In these two simulations, the fitness functions for maximizing irradiance on panels and minimizing illuminance above 3000 lux showed clear

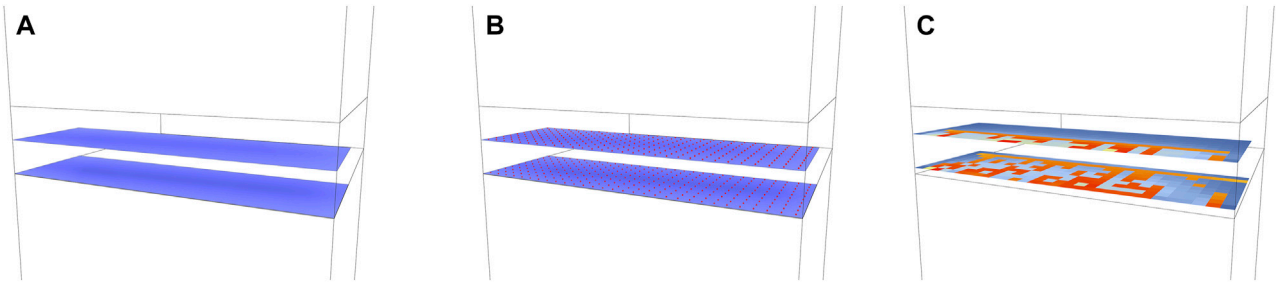

FIGURE 5
The step-by-step construction of the internal space in the primitive phenotype.

TABLE 2 The simulation and algorithm settings of the MOEA.

Weather data		Sydney (33.8688°S, 151.2093°E) EPW file	
Simulation tool		Ladybug, Honeybee V. 1.5	
Analysis tool		Wallacei	
Simulation time		A typical summer day (21.06) at 8 a.m., 12 p.m., 4 p.m.	
Analysis grid		1.2*1.2 m^2	
Material reflectance and transmittance		Facade: 0.35, PV: 0.05, glazing: 0.88	
Simulation size		Algorithm settings	
Generation size/count	35/140	Mutation rate	1/n (*n* = no. of var.)
Population size	4900	Crossover probability	0.9
No. of chromosomes	1	Mutation distribution index	20
No. of variables	6264	Crossover distribution index	20
Size of search space	4.4×10^{139}	Algorithm runtime	112 h., 20 min, 50 s

indication of convergence towards an optimal solution, (with the 12 p.m. simulation demonstrating better convergence than the 4 p.m. simulation), however due to the conflicting nature of the fitness functions, in both simulations, the algorithm struggled to converge the third fitness function that minimizes illuminance below 300 lux.

This conflict indicates that the algorithm has found it more efficient to optimize for irradiance on solar panels and minimize illuminance above 3000 lux than to minimize illuminance below 300 lux. It is important to note that despite the algorithm's inability to converge the third fitness function towards an optimal solution, a further analysis of the results showcase successful results for this fitness function.

Due to the conflicting nature of the fitness functions being optimized for in each simulation, there is no single optimal solution that is generated by the algorithm, as what is optimal for one fitness function, may not be for another. Instead of outputting a single optimal solution, the algorithm outputs a solution set that forms part of the "Pareto Front." The solutions in the Pareto Front are the "best" solutions evolved by the algorithm, in which no solution can be improved without making another solution on the Pareto Front worse. In each of the three simulations (8 a.m., 12 p.m., 4 p.m.), the Pareto Front consisted of 14 solutions, 46 solutions, and 85 solutions respectively. To capture the variation of solutions across the Pareto Front, two types of solutions were selected from each simulation for further analysis; the outlier solutions, which are the most optimal solutions for each fitness function separately; and the "Utopia" solution, which is the solution that is closest to the 'ideal' solution (defined as the solution that is impossible to achieve due to the conflict between the fitness functions) (Showkatbakhsh and Mohammed, 2022) (Figure 7).

5 Discussion

This research revolves through three main objectives using a BIPV shading system:

- Minimum over lit spots with an illuminance above 3000 lux.
- Minimum underlit spots with an illuminance under 300 lux to increase visual comfort.
- Maximum irradiation (W/m2) on PV cells to increase energy generation potentials.

Accordingly, a MOEA is employed to represent the most efficient design considering either one of the objectives (the outlier solutions) or all together (Utopia solution). Figure 8

FIGURE 6
The results of the MOEA. Each set of charts corresponds to a different simulation: from top to bottom, 8 a.m., 12 p.m., and 4 p.m. The charts present the fitness values for every solution in the population through different graphical analyses. From left to right: Standard Deviation chart presents the variation and mean of each generation (the red to blue color scheme represents the first to last generation). The second chart is the fitness values chart, which presents each solution evolved by the population; each line on this chart represents a generation and each point on the line represents a solution in that generation. Finally, the third and fourth charts represent the variation and average of each generation respectively across all 140 generations.

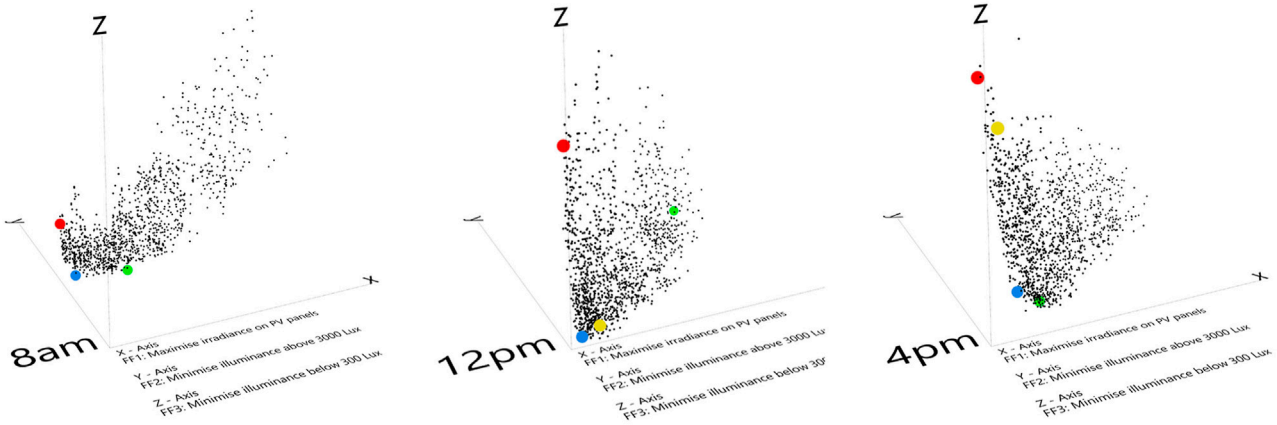

FIGURE 7
The solutions of each simulation distributed in the objective space to present the relationship between solutions and spread of fitness values across the entire population. The outlier solutions are highlighted (red highlights most optimal solution for irradiance on PV panels, green highlights the most optimal solution for minimizing lux below 300, and yellow highlights the most optimal solution for minimizing lux above 3000) as well as the Utopia solutions (the solution closest to the 'ideal' point, which in the presented charts is located on the 0,0,0 point of the graph. The Utopia point is highlighted in blue).

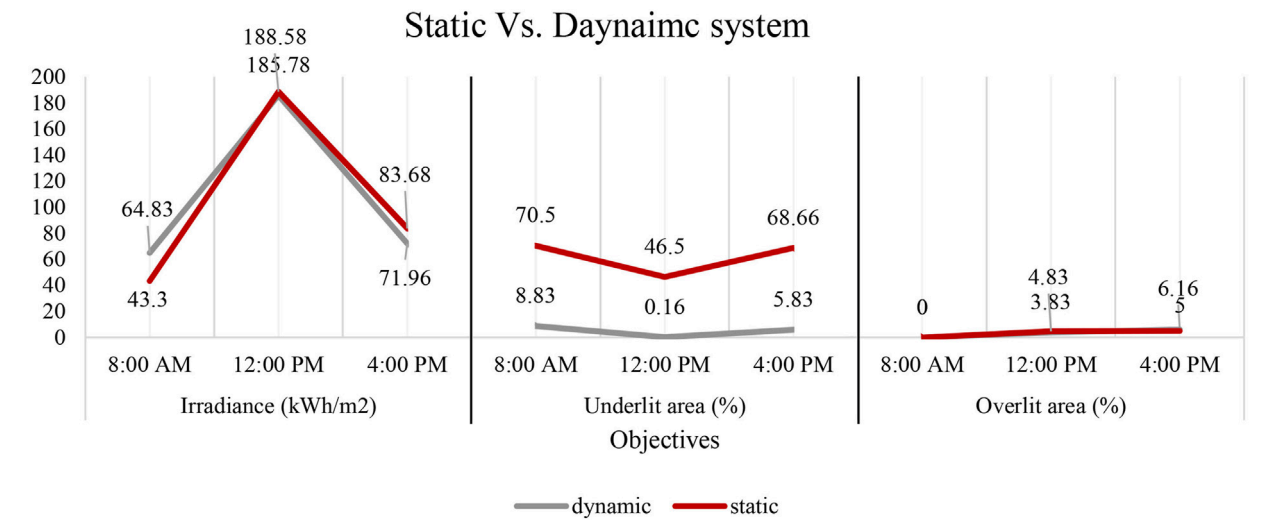

FIGURE 8
A comparison of static and Dynamic BIPV systems' performance.

presents the selected phenotypes from each simulation (the outliers and Utopia solution) with each solution's fitness values and the relationship between the fitness values as visualized through the diamond chart under each phenotype. As can be observed (Table 3), the Utopia solution identifies the solution that most equally optimizes for all fitness functions, while the outlier solutions prioritize the optimization of their respective fitness function, thus highlighting the conflict to the remaining fitness functions. The comparative analysis between the outliers and Utopia solution is vital in the presented study; although the natural progression towards selection is to choose the Utopia solution (as its the solution that most evenly optimizes for all fitness functions), the problem at hand presents a strong argument to utilize all the outlier solutions as they present valid configurations for the photovoltaics that respond to a specific time of day and a specific activity taking place inside the space being analyzed. In the case of the presented results, in each of the three simulations, the outlier that favors irradiance on the PVs is the most suitable panel configuration in the hours that the internal space is not inhabited (for example, before or after working hours or on weekends), as there is minimal need to ensure specific lux values are maintained during these uninhabited hours. Whereas in instances where the space is inhabited, the Utopia solution is more suitable as it evenly balances between irradiance on PVs as well as lux values in the interior spaces. This adaptability and reconfiguration of PVs throughout the day, an affordance provided by an alternative approach to static PV panels as facade systems,

10.3389/fbuil.2023.1119696

TABLE 3 The Outlier and Utopia solution and their associated fitness values for each simulation.

8:00 am	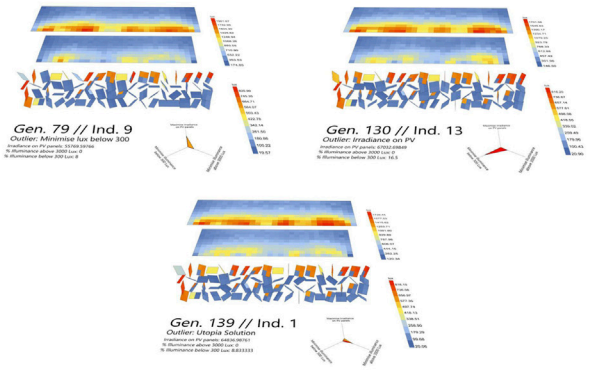	Outlier 1 (Best Solution for lux below 300) Solution Location: Gen 79 / Ind 9 Irradiance: 55.76 kWh/m2 % below 300 lux: 8.00 % above 3000 lux: 0.00 Outlier 2 (Best Solution for Irradiance) Solution Location: Gen 130 / Ind 13 Irradiance: 67.03 kWh/m2 % below 300 lux: 16.50 % above 3000 lux: 0.00 Utopia Solution Solution Location: Gen 139 / Ind 1 Irradiance: 64.83 kWh/m2 % below 300 lux: 8.83 % above 3000 lux: 0.00
12:00 pm	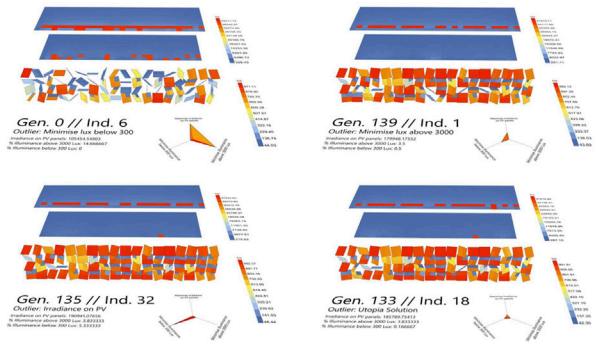	Outlier 1 (Best Solution for lux below 300) Solution Location: Gen 0 / Ind 6 Irradiance: 105.45 kWh/m2 % below 300 lux: 0.00 % above 3000 lux: 14.67 Outlier 2 (Best Solution for lux above 3000) Solution Location: Gen 139 / Ind 1 Irradiance: 179.94 kWh/m2 % below 300 lux: 0.50 % above 3000 lux: 3.50 Outlier 3 (Best Solution for Irradiance) Solution Location: Gen 135 / Ind 32 Irradiance: 190.94 kWh/m2 % below 300 lux: 5.33 % above 3000 lux: 3.83 Utopia Solution Solution Location: Gen 133 / Ind 18 Irradiance: 185.78 kWh/m2 % below 300 lux: 0.17 % above 3000 lux: 3.83
4:00 pm	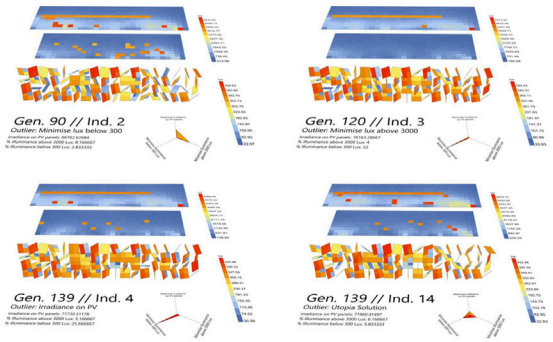	Outlier 1 (Best Solution for lux below 300) Solution Location: Gen 90/ Ind 2 Irradiance: 66.76 kWh/m2 % below 300 lux: 2.83 % above 3000 lux: 8.17 Outlier 2 (Best Solution for lux above 3000) Solution Location: Gen 120 / Ind 3 Irradiance: 76.16 kWh/m2 % below 300 lux: 22.00 % above 3000 lux: 4.00 Outlier 3 (Best Solution for Irradiance) Solution Location: Gen 139 / Ind 4 Irradiance: 77.73 kWh/m2 % below 300 lux: 25.67 % above 3000 lux: 5.17 Utopia Solution Solution Location: Gen 139 / Ind 14 Irradiance: 71.96 kWh/m2 % below 300 lux: 5.83 % above 3000 lux: 6.17

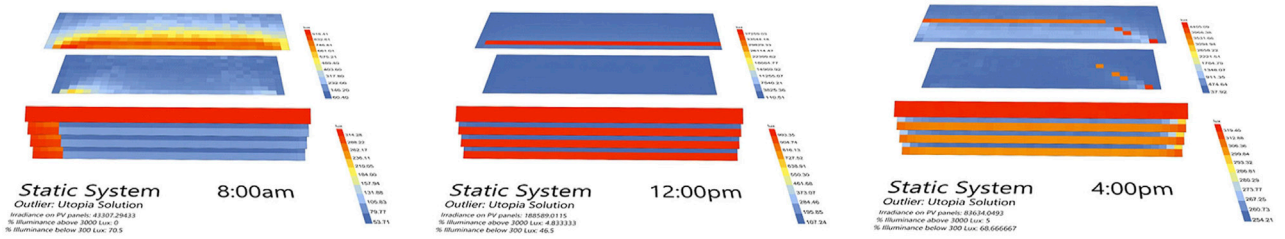

FIGURE 9
Static BIPV shading system performance (indoor illuminance and outdoor irradiation).

coupled with multi-objective optimization algorithms, is critical to increasing efficiency of solar exposure throughout different times of the day.

Meanwhile, a 60-degree tilted static system showed a weak performance, especially with regards to reducing underlit spots with an illuminance lower than 300 lux. In other words, as shown in Figure 8, an average daily of 56.94% difference in the minimum threshold level of illuminance is observed between static and dynamic BIPV shading system. This is while energy generation potentials in dynamic system reaches to its maximum (increasing 21.53%) in the morning (at 8 a.m.) with an average daily improvement percentage of 2.35%, compared to the static one. The spatial percentage of area with an illuminance over 3000 lux, which increases visual discomfort and glare probability is also alleviated by up to 1.16% in the dynamic system.

The spatial distribution of underlit and overlit interior spots and irradiation on fixed PV panels for different times of the day (8 a.m., 12 p.m., 4 p.m.) is shown in Figure 9.

Fixed static shading systems, not only have shown a lower performance regarding both energy generation potentials and visual comfort but also can block outward views, which directly affects occupants' health and wellbeing. Although dynamic systems have a higher installation and maintenance cost, they offer numerous advantages to users and investors. For example, another benefit of dynamic systems is that they can control direct and indirect radiations, which balances solar heat gain and loss in extreme seasons (winter and summer) (Jayathissa et al., 2017), and eventually brings comfort to the occupants and reduces the annual energy demand of buildings.

6 Conclusion

This research aims to show the importance of adopting a multi-functional real-time adaptive BIPV system as a response to climate change and associated energy use augments. To support this suggestion, a real-time adaptive BIPV shading system is designed and evaluated with the use of multi-objective evolutionary computation methods. This multi-objective study operated on extracting optimal BIPV façade configurations while addressing three fitness functions simultaneously: To maximize irradiance value on the BIPV, minimize internal illuminance values above 3000 lux, and minimize internal illuminance levels below 300 lux, thus increasing visual comfort in building interiors, minimizing underlit and overlit spots, and maximizing energy generation potential of the BIPV façade. The performance comparison of the real-time adaptive BIPV façade solution with typical static BIPV panel installations revealed the benefits of the proposed adaptive system considering its attainment of optimum visual comfort conditions and energy generation potential irrespective of the time of the day. This aspect is seen as a substantial achievement considering the limitations of a static BIPV system with regards to its exposure to solar irradiation and limited adaptive ability towards visual comfort.

The proposed multi-objective evolutionary computing method and the resulting real-time adaptive BIPV façade solution can certainly be used for proposed new-built scenarios, and for existing building stock, in the form of a retrofitting initiative. The adoption of such retrofit processes will be beneficial to occupants, investors, and the climatic context alike resulting in economic, health, and environmental benefits. Moreover, there is an opportunity to establish an interactive model between the inhabitants and the BIPV system (similar to an inhabitant's interaction with a HVAC system) where the inhabitants can control internal illuminance comfort levels through choosing from a pre-defined set of BIPV configurations at different times throughout the day. The research findings thus profess an integrated approach wherein computational tools and techniques can aid in the multi-performative deployment of BIPV systems, thus contributing towards on-going efforts to mitigate climate change and maximizing renewable energy use potential.

Data availability statement

The raw data supporting the conclusion of this article will be made available by the authors, without undue reservation.

Author contributions

Methodology, NB, MM, NA; Case Study, MM; Analysis, MM, NA; Writing-original draft preparation, NB, MM, NA; Writing-review and editing, NB, MM, NA.

Conflict of interest

The authors declare that the research was conducted in the absence of any commercial or financial relationships that could be construed as a potential conflict of interest.

Publisher's note

References

Agathokleous, R. A., and Kalogirou, S. A. (2016). Double skin facades (DSF) and building integrated photovoltaics (BIPV): A review of configurations and heat transfer characteristics. *Renew. Energy* 89, 743–756. doi:10.1016/j.renene.2015.12.043

Abdollahzadeh, N., and Biloria, N. (2022). Urban microclimate and energy consumption: A multi-objective parametric urban design approach for dense subtropical cities. *Front. Archit. Res.*, 1–13. doi:10.1016/j.foar.2022.02.001

Australian Building Codes Board (2016). *National construction code volume one. Building code of Australia, class 2 to class 9 buildings*. Canberra: Australian Building Codes Board.

Bahr, W. (2014). A comprehensive assessment methodology of the building integrated photovoltaic blind system. *Energy Build.* 82, 703–708. doi:10.1016/j.enbuild.2014.07.065

Biloria, N., and Abdollahzadeh, N. (2022). "Energy-efficient retrofit measures to achieve nearly zero energy buildings." In *Nearly zero energy building (NZEB) - materials, design and new approaches*, London, UK: IntechOpen. doi:10.5772/intechopen.101845

Biyik, E., Araz, M., Hepbasli, A., Shahrestani, M., Yao, R., Shao, L., et al. (2017). A key review of building integrated photovoltaic (BIPV) systems. *Eng. Sci. Technol. Int. J.* 20, 833–858. doi:10.1016/j.jestch.2017.01.009

Bonomo, P., Chatzipanagi, A., and Frontini, F. (2015). Overview and analysis of current BIPV products: New criteria for supporting the technological transfer in the building sector. *Vitr. J. Archit. Technol. Sustain.* 2015, 67–85. doi:10.4995/vitruvio-ijats.2015.4476

Cannavale, A., Ierardi, L., Hörantner, M., Eperon, G. E., Snaith, H. J., Ayr, U., et al. (2017). Improving energy and visual performance in offices using building integrated perovskite-based solar cells: A case study in southern Italy. *Appl. Energy* 205, 834–846. doi:10.1016/j.apenergy.2017.08.112

Chae, Y. T., Kim, J., Park, H., and Shin, B. (2014). Building energy performance evaluation of building integrated photovoltaic (BIPV) window with semi-transparent solar cells. *Appl. Energy* 129, 217–227. doi:10.1016/j.apenergy.2014.04.106

Chi, A., Rangel, D., and Navarro, J. (2018). Correlating daylight availability metric with lighting, heating, and cooling energy consumptions. *Build. Environ.* 132, 170–180. doi:10.1016/j.buildenv.2018.01.048

Council of Australian Governments (COAG) (2012). Baseline energy consumption and greenhouse gas emissions.

Davidsson, H., Perers, B., and Karlsson, B. (2010). Performance of a multifunctional PV/T hybrid solar window. *Sol. Energy* 84, 365–372. doi:10.1016/j.solener.2009.11.006

Davidsson, H., Perers, B., and Karlsson, B. (2012). System analysis of a multifunctional PV/T hybrid solar window. *Sol. Energy* 86, 903–910. doi:10.1016/j.solener.2011.12.020

Deb, K., Agrawal, S., Pratap, A., and Meyarivan, T. (2000). "A fast elitist non-dominated sorting genetic algorithm for multi-objective optimization: NSGA-II," in *International conference on parallel problem solving from nature*: Springer, 849–858.

De Jong, K. A. (2006). *Evolutionary computation: A unified approach*. Massachusetts, United States: MIT Press.

Defaix, P. R., Van Sark, W., Worrell, E., and de Visser, E. (2012). Technical potential for photovoltaics on buildings in the EU-27. *Sol. Energy* 86, 2644–2653. doi:10.1016/j.solener.2012.06.007

Delponte, E., Marchi, F., Frontini, F., Polo, C., Fath, K., and Batey, M. (2015). "BIPV in EU28, from niche to mass market: An assessment of current projects and the potential for growth through product innovation," in Proceedings of the 31st European Photovoltaic Solar Energy Conference and Exhibition, Hamburg, Germany, 14-18 September 2015, 3046–3050.

Dewidar, K., Mahmoud, A. H., Magdy, N., and Ahmed, S. (2010). "The role of intelligent façades in energy conservation Khaled," in Proceeding Int. Conf. Sustain. Futur. Futur. Intermed. sus- tainable cities, Egypt.

Eicker, U., Demir, E., and Gürlich, D. (2015). Strategies for cost efficient refurbishment and solar energy integration in European Case Study buildings. *Energy Build.* 102, 237–249. doi:10.1016/j.enbuild.2015.05.032

Ernstand Young (2016). *The Upside of Disruption: Megatrends shaping 2016 and beyond*.

Evola, G., and Margani, G. (2016). Renovation of apartment blocks with BIPV: Energy and economic evaluation in temperate climate. *Energy Build.* 130, 794–810. doi:10.1016/j.enbuild.2016.08.085

Farkas, K., Frontini, F., Maturi, L., Munari Probst, M. C., Roecker, C., and Scognamiglio, A. (2013). *Designing photovoltaic systems for architectural integration*. France: Farkas, Klaudia pour International Energy Agency Solar Heating and Cooling.

Fossa, M., Ménézo, C., and Leonardi, E. (2008). Experimental natural convection on vertical surfaces for building integrated photovoltaic (BIPV) applications. *Exp. Therm. fluid Sci.* 32, 980–990. doi:10.1016/j.expthermflusci.2007.11.004

Freitas, S., and Brito, M. C. (2015). "Maximizing the solar photovoltaic yield in different building facade layouts," in Proceedings of the European Photovoltaic Solar Energy Conference and Exhibition, Hamburg, Germany, 14-18 September 2015, 14–18.

Gao, Y., Dong, J., Isabella, O., Santbergen, R., Tan, H., Zeman, M., et al. (2018). A photovoltaic window with sun-tracking shading elements towards maximum power generation and non-glare daylighting. *Appl. Energy* 228, 1454–1472. doi:10.1016/j.apenergy.2018.07.015

Gonçalves, J. E., van Hooff, T., and Saelens, D. (2020). Understanding the behaviour of naturally-ventilated BIPV modules: A sensitivity analysis. *Renew. Energy* 161, 133–148. doi:10.1016/j.renene.2020.06.086

Hachem, C., Athienitis, A., and Fazio, P. (2014). Energy performance enhancement in multistory residential buildings. *Appl. Energy* 116, 9–19. doi:10.1016/j.apenergy.2013.11.018

Heidari Matin, N., and Eydgahi, A. (2019). Technologies used in responsive facade systems: A comparative study. *Intell. Build. Int.* 2019, 54–73. doi:10.1080/17508975.2019.1577213

Hong, T., Koo, C., Oh, J., and Jeong, K. (2017). Nonlinearity analysis of the shading effect on the technical–economic performance of the building-integrated photovoltaic blind. *Appl. Energy* 194, 467–480. doi:10.1016/j.apenergy.2016.05.027

IEA (2019). *Renewables 2019: Analysis and forecasts to 2024*. Paris: Int. Energy Agency.

International Energy Agency (2013). *Renewable energy medium-term market report – market trends and projections to 2018*. Paris, France: International Energy Agency.

Jayathissa, P., Luzzatto, M., Schmidli, J., Hofer, J., Nagy, Z., and Schlueter, A. (2017). Optimising building net energy demand with dynamic BIPV shading. *Appl. Energy* 202, 726–735. doi:10.1016/j.apenergy.2017.05.083

Jelle, B. P., Breivik, C., and Røkenes, H. D. (2012). Building integrated photovoltaic products: A state-of-the-art review and future research opportunities. *Sol. Energy Mat. Sol. Cells* 100, 69–96. doi:10.1016/j.solmat.2011.12.016

Jeong, K., Hong, T., Koo, C., Oh, J., Lee, M., and Kim, J. (2017). A prototype design and development of the smart photovoltaic system blind considering the photovoltaic panel, tracking system, and monitoring system. *Appl. Sci.* 7, 1077. doi:10.3390/app7101077

Joe, J., Choi, W., Kwon, H., and Huh, J.-H. (2013). Load characteristics and operation strategies of building integrated with multi-story double skin facade. *Energy Build.* 60, 185–198. doi:10.1016/j.enbuild.2013.01.015

Kaelin, M., Rudmann, D., and Tiwari, A. N. (2004). Low-cost processing of CIGS thin film solar cells. *Sol. Energy* 77, 749–756. doi:10.1016/j.solener.2004.08.015

Kang, S., Hwang, T., and Kim, J. T. (2012). Theoretical analysis of the blinds integrated photovoltaic modules. *Energy Build.* 46, 86–91. doi:10.1016/j.enbuild.2011.10.042

Karava, P., Jubayer, C. M., Savory, E., and Li, S. (2012). Effect of incident flow conditions on convective heat transfer from the inclined windward roof of a low-rise building with application to photovoltaic-thermal systems. *J. Wind Eng. Ind. Aerodyn.* 104, 428–438. doi:10.1016/j.jweia.2012.03.026

Kolarevic, B., and Parlac, V. (2015). Building dynamics: Exploring architecture of change. *Build. Dyn. Explor. Archit. Chang.* 2015, 1–298. doi:10.4324/9781315763279

Koo, C., Hong, T., Jeong, K., Ban, C., and Oh, J. (2017). Development of the smart photovoltaic system blind and its impact on net-zero energy solar buildings using technical-economic-political analyses. *Energy* 124, 382–396. doi:10.1016/j.energy.2017.02.088

Kushiya, K. (2014). CIS-based thin-film PV technology in solar frontier KK. *Sol. Energy Mat. Sol. Cells* 122, 309–313. doi:10.1016/j.solmat.2013.09.014

Lee, E., Selkowitz, S., Bazjanac, V., Inkarojrit, V., and Kohler, C., 2002. High-performance commercial building façades.Report LBNL-50502

Loonen, R. C. G. M., Trčka, M., Cóstola, D., and Hensen, J. L. M. (2013). Climate adaptive building shells: State-of-the-art and future challenges. *Renew. Sustain. energy Rev.* 25, 483–493. doi:10.1016/j.rser.2013.04.016

Lucon, O., and Ürge-Vorsatz, D. (2014). Fifth assessment report, mitigation of climate change. *Intergov. Panel Clim. Chang.*, 674–738.

Luo, Y., Zhang, L., Liu, Z., Xie, L., Wang, X., and Wu, J. (2018). Experimental study and performance evaluation of a PV-blind embedded double skin façade in winter season. *Energy* 165, 326–342. doi:10.1016/j.energy.2018.09.175

Luo, Y., Zhang, L., Wang, X., Xie, L., Liu, Z., Wu, J., et al. (2017). A comparative study on thermal performance evaluation of a new double skin façade system integrated with photovoltaic blinds. *Appl. Energy* 199, 281–293. doi:10.1016/j.apenergy.2017.05.026

Makki, M., Showkatbakhsh, M., and Song, Y. (2018). *Wallacei, An evolutionary and analytic engine for Grasshopper 3D, Primer 2.0*.

Martín-Chivelet, N., Gutiérrez, J. C., Alonso-Abella, M., Chenlo, F., and Cuenca, J. (2018). Building retrofit with photovoltaics: Construction and performance of a BIPV ventilated façade. *Energies* 11, 1719. doi:10.3390/en11071719

Nielsen, M. V., Svendsen, S., and Jensen, L. B. (2011). Quantifying the potential of automated dynamic solar shading in office buildings through integrated simulations of energy and daylight. *Sol. Energy* 85, 757–768. doi:10.1016/j.solener.2011.01.010

Palmero-Marrero, A. I., and Oliveira, A. C. (2010). Effect of louver shading devices on building energy requirements. *Appl. Energy* 87, 2040–2049. doi:10.1016/j.apenergy.2009.11.020

Park, H. S., Koo, C., Hong, T., Oh, J., and Jeong, K. (2016). A finite element model for estimating the techno-economic performance of the building-integrated photovoltaic blind. *Appl. Energy* 179, 211–227. doi:10.1016/j.apenergy.2016.06.137

Paydar, M. A. (2020). Optimum design of building integrated PV module as a movable shading device. *Sustain. Cities Soc.* 62, 102368. doi:10.1016/j.scs.2020.102368

Peng, J., Curcija, D. C., Lu, L., Selkowitz, S. E., Yang, H., and Zhang, W. (2016). Numerical investigation of the energy saving potential of a semi-transparent photovoltaic double-skin facade in a cool-summer Mediterranean climate. *Appl. Energy* 165, 345–356. doi:10.1016/j.apenergy.2015.12.074

Peng, J., Lu, L., Yang, H., and Han, J. (2013). Investigation on the annual thermal performance of a photovoltaic wall mounted on a multi-layer façade. *Appl. Energy* 112, 646–656. doi:10.1016/j.apenergy.2012.12.026

Poon, K. H., Kämpf, J. H., Tay, S. E. R., Wong, N. H., and Reindl, T. G. (2020). Parametric study of URBAN morphology on building solar energy potential in Singapore context. *Urban Clim.* 33, 100624. doi:10.1016/j.uclim.2020.100624

Prieto, A., Knaack, U., Auer, T., and Klein, T. (2019). Coolfacade: State-of-the-art review and evaluation of solar cooling technologies on their potential for façade integration. *Renew. Sustain. Energy Rev.* 101, 395–414. doi:10.1016/j.rser.2018.11.015

Quesada, G., Rousse, D., Dutil, Y., Badache, M., and Hallé, S. (2012). A comprehensive review of solar facades. Transparent and translucent solar facades. *Renew. Sustain. Energy Rev.* 16, 2643–2651. doi:10.1016/j.rser.2012.02.059

Raugei, M., and Frankl, P. (2009). Life cycle impacts and costs of photovoltaic systems: Current state of the art and future outlooks. *Energy* 34, 392–399. doi:10.1016/j.energy.2009.01.001

Roudsari, M. S., and Mackey, C. (2012). Ladybug Tools (1.5) [WWW Document]. Ladybug Tools. Available at: https://www.ladybug.tools/.

Secretariat, U. (2015). "United Nations framework convention on climate change," in Report of the Conference of the Parties on its twenty-first session, Paris, 30 November to 13 December 2015.

Showkatbakhsh, M., and Mohammed, M. (2022). Multi-objective optimisation of urban form: A framework for selecting the optimal solution. *Build. (Basel).* 12 (9), 1473. doi:10.3390/buildings12091473

Sun, L., Lu, L., and Yang, H. (2012). Optimum design of shading-type building-integrated photovoltaic claddings with different surface azimuth angles. *Appl. Energy* 90, 233–240. doi:10.1016/j.apenergy.2011.01.062

Taveres-Cachat, E., Lobaccaro, G., Goia, F., and Chaudhary, G. (2019). A methodology to improve the performance of PV integrated shading devices using multi-objective optimization. *Appl. Energy* 247, 731–744. doi:10.1016/j.apenergy.2019.04.033

Vadiee, A., Yaghoubi, M., Martin, V., and Bazargan-Lari, Y. (2016). Energy analysis of solar blind system concept using energy system modelling. *Sol. Energy* 139, 297–308. doi:10.1016/j.solener.2016.09.039

Wpcpey (2017). UTS tower building 201708 [WWW Document]. Available at: https://commons.wikimedia.org/wiki/File:UTS_Tower_Building_201708.jpg (Accessed Febuary 23 2023).

Wilson, G. (2015). Cell efficiency records. Availabe at:http://www.nrel.gov/ncpv/.

Yang, S., Cannavale, A., Di Carlo, A., Prasad, D., Sproul, A., and Fiorito, F. (2020). Performance assessment of BIPV/T double-skin façade for various climate zones in Australia: Effects on energy consumption. *Sol. Energy* 199, 377–399. doi:10.1016/j.solener.2020.02.044

Yang, T., and Athienitis, A. K. (2016). A review of research and developments of building-integrated photovoltaic/thermal (BIPV/T) systems. *Renew. Sustain. Energy Rev.* 66, 886–912. doi:10.1016/j.rser.2016.07.011

Yoo, S. H., and Manz, H. (2011). Available remodeling simulation for a BIPV as a shading device. *Sol. Energy Mat. Sol. Cells* 95, 394–397. doi:10.1016/j.solmat.2010.02.015

Yoo, S. H. (2011). Simulation for an optimal application of BIPV through parameter variation. *Sol. Energy* 85, 1291–1301. doi:10.1016/j.solener.2011.03.004

Yu, G., Yang, H., Luo, D., Cheng, X., and Ansah, M. K. (2021). A review on developments and researches of building integrated photovoltaic (BIPV) windows and shading blinds. *Renew. Sustain. Energy Rev.* 149, 111355. doi:10.1016/j.rser.2021.111355